



**HAL**  
open science

## Seismicity in sheared granular matter

Aghil Abed Zadeh, Jonathan Barés, Joshua E S Socolar, Robert Behringer

► **To cite this version:**

Aghil Abed Zadeh, Jonathan Barés, Joshua E S Socolar, Robert Behringer. Seismicity in sheared granular matter. *Physical Review E* , 2019, 99, pp.052902. 10.1103/PhysRevE.99.052902 . hal-02137063

**HAL Id: hal-02137063**

**<https://hal.science/hal-02137063v1>**

Submitted on 22 May 2019

**HAL** is a multi-disciplinary open access archive for the deposit and dissemination of scientific research documents, whether they are published or not. The documents may come from teaching and research institutions in France or abroad, or from public or private research centers.

L'archive ouverte pluridisciplinaire **HAL**, est destinée au dépôt et à la diffusion de documents scientifiques de niveau recherche, publiés ou non, émanant des établissements d'enseignement et de recherche français ou étrangers, des laboratoires publics ou privés.

# Seismicity in sheared granular matter

Aghil Abed Zadeh,<sup>1,\*</sup> Jonathan Barés,<sup>2</sup> Joshua E. S. Socolar,<sup>1</sup> and Robert P. Behringer<sup>1,†</sup>

<sup>1</sup>*Department of Physics & Center for Non-linear and Complex Systems, Duke University, Durham, North Carolina 27708, USA*

<sup>2</sup>*Laboratoire de Mécanique et Génie Civil, Université de Montpellier, CNRS, Montpellier, France*

We report on experiments investigating the dynamics of a slider that is pulled by a spring across a granular medium consisting of a vertical layer of photoelastic disks. The motion proceeds through a sequence of discrete events, analogous to seismic shocks, in which elastic energy stored in the spring is rapidly released. We measure the statistics of several properties of the individual events: the energy loss in the spring, the duration of the movement, and the temporal profile of the slider motion. We also study certain conditional probabilities and the statistics of mainshock-aftershock sequences. At low driving rates, we observe crackling with Omori-Utsu, Båth, and waiting time laws similar to those observed in seismic dynamics. At higher driving rates, where the sequence of events shows strong periodicity, we observe scaling laws and asymmetrical event shapes that are clearly distinguishable from those in the crackling regime.

## I. INTRODUCTION

A wide variety of physical systems exhibit stick-slip dynamics in response to a steady driving force. In such systems, configurations of microscopic elements remain stable as the force builds up, then undergo fast microscopic rearrangements during macroscopic relaxation events. When the driving force is increased slowly, the distribution of event sizes often develops a power-law form, and the system is said to “crackle” [1]. Examples can be found in phenomena associated with fracture [2–5], friction [6,7], magnetization [8], neural activity [9,10], and seismicity [5,11,12], to mention a few.

Many experimental studies [13–19], simulations [17,20–23], and theoretical models [24–27] have investigated the statistics of sizes and durations of slip events in disordered athermal systems. Such studies typically focus on the quasistatic regime, where the driving rate is slower than any relevant intrinsic time scale. Several conceptual tools for characterizing the dynamics were originally developed for the purpose of analyzing seismological data and forecasting earthquakes. In that context, it has been observed that the statistics of mainshocks (MS) and aftershocks (AS) follow several phenomenological scaling laws [28]: the Gutenberg-Richter power-law decay in the event size distribution; a power-law distribution of the waiting times between successive events [5,11,29]; a power-law distribution of AS productivity as a function of MS magnitude [30,31]; Båth’s law [32] for the constancy of the size ratio of the largest AS to the MS that produced it; and the Omori-Utsu law [33–35] for the decay in the rate of AS following a given MS. These laws, referred to as the fundamental laws of seismology [36], are used in the probabilistic forecasting of earthquakes, and it is important to understand their mechanistic origins and potential applicability to other types of crackling phenomena.

This paper reports on experimental studies of a slider that is pulled over a granular material. The system resembles earthquake systems in that stress accumulates at a slow, constant rate due to an external driving mechanism and is released rapidly in discrete events. Moreover, the granular matter (gouge) between two tectonic plates may play an important role in earthquake dynamics, which motivates us to probe the dynamics induced by the granular matter alone, in the absence of appreciable elastic deformations of the plates themselves. Krim *et al.* have also noted the importance of vibrations in determining frictional properties of granular materials, employing an apparatus quite similar to ours to study the statistics of events for a slider pulled at a given speed while vibrating at various frequencies [37]. The present work focuses on the zero vibration case and the dependence of event statistics on the pulling speed.

Our system undergoes a transition from crackling to periodic dynamics as the driving rate is increased [38]. We present results for all of the statistical quantities mentioned above in both regimes. We find that for slow driving rates our system follows familiar seismic laws and their associated predictions. For higher driving rates, however, the statistics of plastic events changes significantly. Our results in the crackling regime can serve as tests for general theories that have been developed in other contexts, such as the theory of epidemic-type aftershock sequences [36,39].

## II. EXPERIMENTAL PROCEDURE

The experimental setup used for the present study is similar to the one used in Refs. [38,40], illustrated schematically in Fig. 1(a). A toothed two-dimensional (2D) frictional slider of length 25 cm and mass 85 g is attached to a linear spring of stiffness  $k = 70$  N/m. The end of the spring is pulled at a constant speed  $c$ . The slider lies on a vertical bed of bi-disperse cylindrical elastic particles of diameters 4 and 5 mm, with the number ratio  $N_{\text{small}}/N_{\text{big}} = 2.7$ . The granular

---

\*aghil.abed.zadeh@duke.edu

†Deceased.

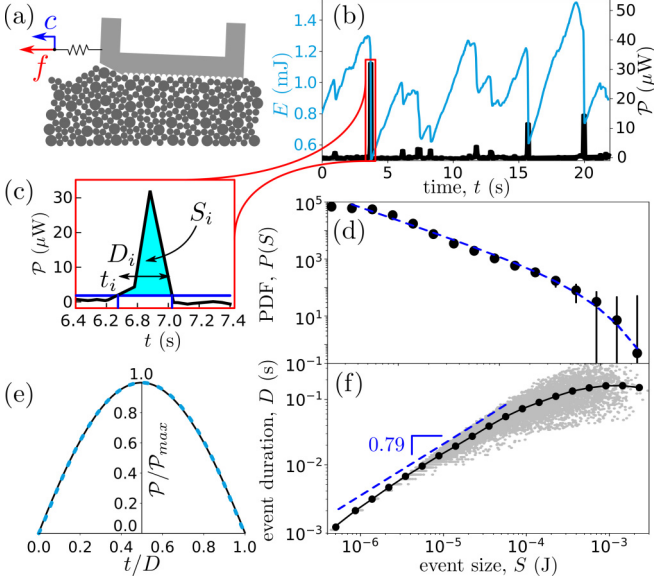


FIG. 1. Stick-slip event statistics for loading speed  $c = 0.1$  mm/s. (a) Schematic of the experiment at loading speed  $c$ . (b) Time series of the spring energy  $E$  (blue) and radiated power  $\mathcal{P}$  (black). (c) An enlarged view of a single peak in  $\mathcal{P}$  with starting time  $t_i$ , duration  $D_i$ , and size  $S_i$ . The horizontal line indicates the threshold used for event detection. (d) PDF of the event sizes. The blue dashed line is a fit to the form of Eq. (1) with  $\beta = 1.22 \pm 0.07$  and  $S_{\max} = 6.1 \times 10^{-4} \pm 0.7 \times 10^{-4}$  J. Error bars show 95% confidence intervals. (e) Average event shape for  $D \in [0.01, 0.02]$  s. The black solid line is computed from the experimental data, and the blue dashed line is a fit to Eq. (2) with  $\sigma = 1.09 \pm 0.02$ . (f) Event duration as a function of event size. Gray dots are individual events; the black line is the binned average. The dashed line shows a power-law corresponding to  $1/\gamma = 0.79$ .

bed and the slider are sandwiched between two dry-lubricated glass plates. The force  $f$  applied to the spring is measured by a sensor at a frequency of 1 kHz. From the time series  $f(t)$ , we calculate the elastic energy stored in the spring,  $E = f^2/(2k)$ , and the power radiated during a given time step,  $\mathcal{P}$ . In our experiments,  $c$  can vary from 0.02 to 100 mm/s.

Slip events, also called plastic events or avalanches, are identified directly from the  $\mathcal{P}(t)$  data. To avoid including transient effects, we consider the force signal only after the slider has moved approximately half of its length. After this point, the signal is seen to oscillate around a well-defined average. For slower pulling speeds, we collect roughly 1000 avalanches per run, and we include several runs in our statistical analysis. For higher speeds, we collect ten runs with roughly 50 slip events per run.

To identify avalanches, we choose a threshold for  $\mathcal{P}$  of  $1.5 \mu\text{W}$ , which is above our rms noise level of  $1.16 \mu\text{W}$ . As illustrated in Fig. 1(c), an avalanche starts when  $\mathcal{P}$  exceeds the threshold and ends when it next drops below the threshold [17,41]. For each event, we extract the starting time  $t_i$ , the duration  $D_i$ , and the event size  $S_i$ , defined as the total energy radiated during the event, and the temporal profile of the power released by the spring,  $\mathcal{P}_i(\tau)$ , for  $\tau \in [0, D_i]$ , where  $\tau = t - t_i$ . We then construct the following statistical quantities: the probability density function (PDF) for event sizes,

$P(S)$ ; the average duration of events of a given size,  $D(S)$ ; and the average scaled event shape for events with  $D_i \in [D - \delta, D + \delta]$ ,  $\overline{\mathcal{P}}_D(u) \equiv \langle \mathcal{P}_i(\tau) / \max(\mathcal{P}_i(\tau)) \rangle_i$ , where  $u = \tau/D_i$ . Finally, we identify the AS's associated with a given MS for the purpose of observing Båth's law, the productivity law, and the Omori-Utsu law.

### III. CRACKLING DYNAMICS

When the slider is pulled very slowly, we observe crackling dynamics, as evidenced for  $c = 0.1$  mm/s by the two decades of power-law decay in  $P(S)$  shown in Fig. 1(d). The PDF is well fit by the Gutenberg-Richter form

$$P(S) \sim S^{-\beta} e^{-\frac{S}{S_{\max}}}, \quad (1)$$

with  $\beta = 1.22 \pm 0.07$  and  $S_{\max} = (6.1 \pm 0.7) \times 10^{-4}$  J. Figure 1(f) shows a scatter plot of the size and duration of individual events. The average curve  $\langle D(S) \rangle$  also exhibits a power law,  $\langle D \rangle \sim S^{1/\gamma}$ , over two decades, with  $1/\gamma = 0.79 \pm 0.03$ . For large events, the average duration appears to saturate.

Figure 1(e) shows the average shape of avalanches with  $D_i \in [0.01, 0.02]$  s, a subset of the events with their size and duration in the power-law regime of Fig. 1(d). Each avalanche has been rescaled vertically by its maximum power radiated and horizontally by its duration. The form of  $\overline{\mathcal{P}}_D(u)$  has been investigated for a variety of amorphous systems [16,17,23,24]. We follow the procedure of Refs. [42] and [3], fitting the average shape to the form

$$\overline{\mathcal{P}}_D(u) = 4[u(1-u)]^\sigma [1 - a(u-1/2)], \quad (2)$$

where  $a$  is an asymmetry parameter. We find  $a = 0$  and  $\sigma = 1.09 \pm 0.02$ . We note that  $\sigma$  differs significantly from the value  $\sigma = \gamma - 1$  predicted in Ref. [42].

### IV. CORRELATIONS BETWEEN EVENTS

We now consider the statistical relations between avalanches. Figure 2(a) shows the waiting time distribution, which would show a simple exponential decay for an uncorrelated Poisson process. Each curve is obtained by setting a lower cutoff size  $S_c$  and compiling the PDF of the times  $\Delta t = t_{j'} - t_j$ , where  $j$  and  $j'$  refer to successive events with  $S > S_c$ . The curves are scaled horizontally by the average waiting time,  $T_c$ , between the included events, which yields a collapse to a single curve that can be fit by a power law with an exponential cutoff [11]:

$$P(\Delta t | S_c) \sim \frac{1}{T_c} u^{-\nu} e^{-\frac{u}{u_{\max}}}, \quad (3)$$

where  $u = \Delta t/T_c$ . We find  $\nu = 1.10 \pm 0.08$  and  $u_{\max} = 3.04 \pm 0.15$ . The dashed line shows the best fit.

Another conventional method for characterizing correlations between events is known as seismicity declustering [5,43]. For any event  $M$  (called the mainshock), associated aftershocks are defined as all subsequent events occurring before the next event larger than  $M$ . The inset of Fig. 2(a) shows the average number,  $N_{AS}$ , of AS associated with MS of a given size,  $S_{MS}$ . We have checked that his productivity law remains unchanged after random shuffling of the sequence of events.

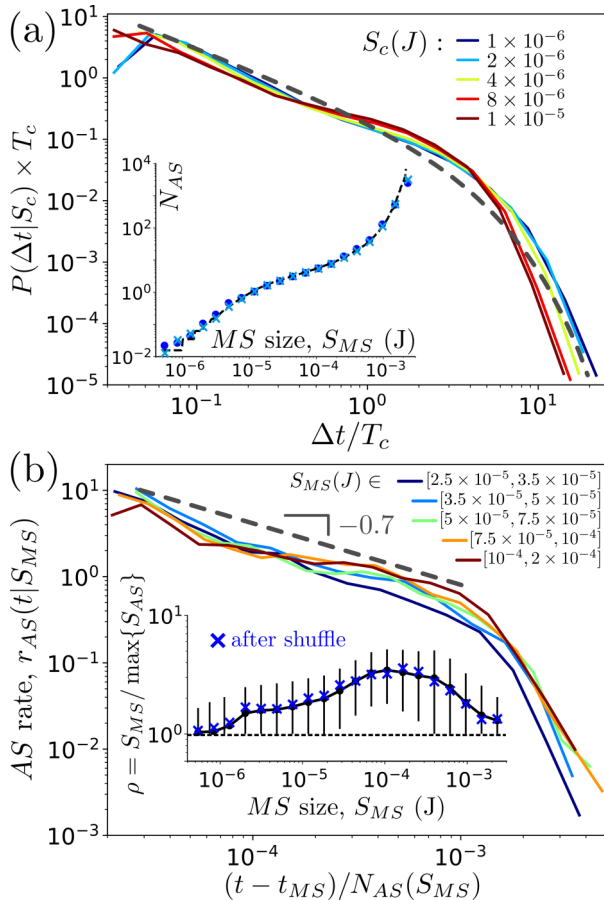


FIG. 2. Waiting time law, productivity law, Omori-Utsu law, and Båth's for  $c = 0.1$  mm/s. (a) Waiting time law: PDF of the waiting time between two consecutive events larger than  $S_c$ , rescaled by  $T_c$ , the average waiting time between events larger than  $S_c$ . The dashed line is a fit to the form of Eq. (3) with  $\nu = 1.10 \pm 0.08$  and  $u_{\max} = 3.04 \pm 0.15$ . Inset: The number of AS's as a function of the MS energy,  $S_{MS}$ . Blue dots are from experiment; cyan crosses are obtained from random permutations of the experimental events, and the black dashed line is obtained from Eq. (4). (b) The rate of AS events corresponding to a MS of energy  $S_{MS}$ . Time is rescaled by  $N_{AS}(S_{MS})$ . The straight dashed line with slope 0.7 is a guide to the eye. Inset: Ratio between MS size,  $S_{MS}$ , and size of the largest AS. Black dots are experimental data; cyan crosses are obtained from a randomly mixed sequence of events.

Given the absence of relevant correlations in the sequence of event sizes, the law can be computed directly from the cumulative event size distributions  $F(S) = \int_{S_{\min}}^S P(s) ds$  [5]:

$$N_{AS}(S_{MS}) = \frac{F(S_{MS})}{1 - F(S_{MS})}. \quad (4)$$

The result, shown as a dashed line in the inset of Fig. 2(a), matches the direct computation, confirming that the sequence of event sizes is essentially random.

Finally, we study the temporal structure of aftershocks, which is characterized by the Omori-Utsu law for the time dependence of the rate  $r$  of aftershock events [33,35] and Båth's law for the ratio  $\rho$  of the size of a MS to its largest AS. Figure 2(b) shows the rate  $r$  of aftershocks following a

MS of size  $S_{MS}$  as a function of the time elapsed since the MS, averaged over MS with similar sizes:  $r$  is a function of  $(t - t_{MS})$ . Curves for different  $S_{MS}$  collapse under the rescaling  $t - t_{MS} \rightarrow (t - t_{MS})/N_{AS}(S_{MS})$  revealing that

$$r(t|S_{MS}) \sim u^{-p} f(u), \quad (5)$$

where  $u = (t - t_{MS})/N_{AS}(S_{MS})$  and  $f$  is a scaling function. We find  $p \approx 0.7$ .

The inset of Fig. 2(b) shows  $\rho$  as a function of  $S_{MS}$ . Within the error bars, the data are consistent with Båth's law, which states that  $\rho = S_{MS}/\max\{S_{AS}\}$  is independent of  $S_{MS}$  and close to 1. Once again, permuting the sequence of events randomly does not change the curve, as shown by blue crosses. This implies that, like productivity law, Båth's law finds its origin in the distribution of individual event sizes, without requiring system memory of the type introduced in epidemic-type aftershock sequence (ETAS) models [36,39].

## V. DRIVING RATE EFFECT

As the driving rate is increased, the system passes into the periodic regime discussed in Ref. [38]. We report here the changes in avalanche statistics associated with this transition. Figure 3(a) shows the evolution of  $P(S)$  with increasing  $c$ . The crackling behavior at low driving rates evolves to a uniform distribution (with an upper cutoff) reaching a stable form for  $c > c_c \approx 20$  mm/s. The inset shows the dependence on  $c$  of the  $P(S)$  exponent,  $\beta$ , indicating that  $\beta \sim \ln(c)$  for  $10^{-1} < c < c_c$ . For faster  $c$ ,  $\beta$  vanishes within the error bars. For slower  $c$  it saturates at a constant value near 1.22.

Figure 3(b) shows the evolution of  $P(\Delta t)$  to a narrow, Gaussian-like distribution for  $c > c_c$  indicating a characteristic time between events. The inset shows the upper cutoff,  $\Delta t_{\max}$ , as a function of  $c$ , revealing a power-law decay for  $c$  slower than  $c_c$ :  $\Delta t_{\max} \sim c^{-0.75 \pm 0.03}$ . For faster  $c$ ,  $\Delta t_{\max}$  decays only logarithmically with increasing  $c$ , as discussed in Ref. [38].

Both  $D(S)$  and  $\overline{P}_D(u)$  for  $D = 0.015$  s show clearly discernible differences in the periodic regime from their crackling behavior at low  $c$ . Figure 4(a) shows  $D(S)$  for different pulling speeds. While  $D(S)$  is a power law in all cases, the exponent is observed to decrease from  $\sim 0.8$  for low  $c$  to  $\sim 0.3$  for  $c > c_c$ .

Figure 4(b) shows how the average event shape of Fig. 1(e) evolves with increasing  $c$ .  $\overline{P}_D(u)$  develops a left-shifted asymmetry as  $c$  increases. The exponent  $\sigma$  and asymmetry parameter  $a$  of Eq. (2) are plotted as a function of  $c$  in the top and bottom insets.  $\sigma$  is roughly constant for low  $c$ , then slowly increases to a saturation value for  $c > c_c$ .  $a$  is near zero for low  $c$  and increases sharply to a constant for  $c > c_c$ , meaning that during the average event in the periodic regime, the slider accelerates faster than it decelerates.

## VI. DISCUSSION

Our experiments demonstrate that slowly shearing a granular bed by means of a pulled slider on its surface gives rise to the same types of scale-free distributions of event sizes, durations, and shapes as those seen in other crackling systems. We

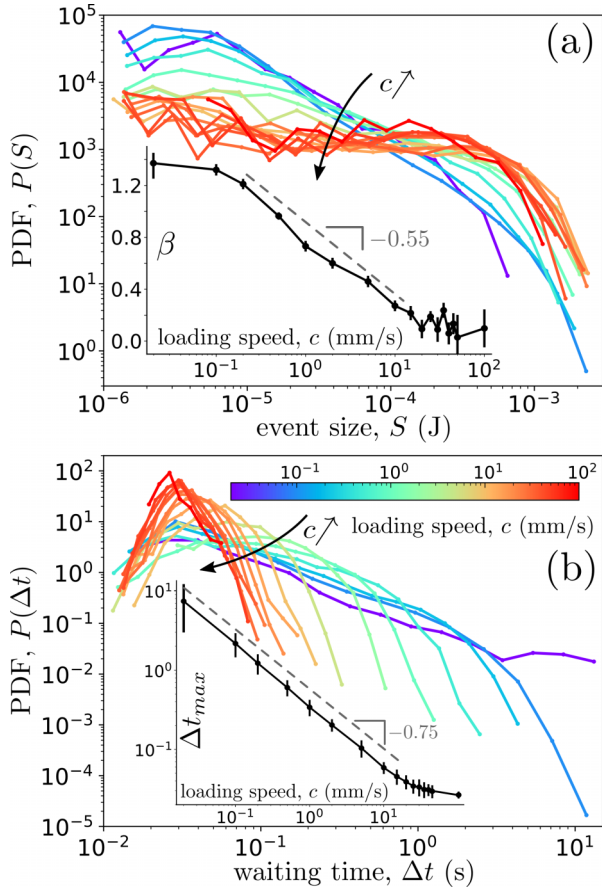


FIG. 3. (a) PDF of the event energy,  $P(S)$ , for loading speeds  $c \in [0.02, 100]$  mm/s. Inset: Logarithmic decay of the exponent  $\beta$  with increasing  $c$ . The fit for  $10^{-1} < c < 20$  mm/s has a slope  $-0.55 \pm 0.06$ . (b) PDF of the waiting time between two consecutive events larger than  $S_c = 10^{-6}$  J for different  $c$ . Inset: Evolution of the upper cutoff,  $\Delta t_{\max}$  [see Eq. (3)] as a function of  $c$ . The fitted power law for  $c < 20$  mm/s shows an exponent of  $-0.75 \pm 0.03$ .

observe behavior that is well described by standard versions of the Gutenberg-Richter law, Omori's law, the productivity law, and Båth's law. As the driving rate is increased, the parameters characterizing the statistics vary smoothly until a crossover occurs to the qualitatively different behavior observed in the periodic regime reported in Ref. [38].

Comparing our results to those from other systems in the crackling regime, we find the following. Our size exponent  $\beta$  matches that observed in many other studies. Several quasi-static theoretical models and simulations [21,23,25–27], as well as fracture experiments by Barés *et al.* [3], reproduce the same scaling exponent within the error bars. This value is smaller, however, than that observed in other dynamic 3D experiments [13,14,16,44] and the mean-field model exponent of 1.5 [16,22,24,29], and it is larger than was found some other studies [20,45]. The exponent  $\gamma$  we measure for the  $D(S)$  power law agrees with 3D experiments of Dalton *et al.* [13] and with dislocation dynamics models [45]. It is lower, however, than those of simulations by Liu *et al.* [23] and a mean-field model by Budrikis *et al.* [26]. Our measured exponent  $\nu$  for the waiting time law agrees with the creep mean-field model [29]. Finally, as has been recently reported

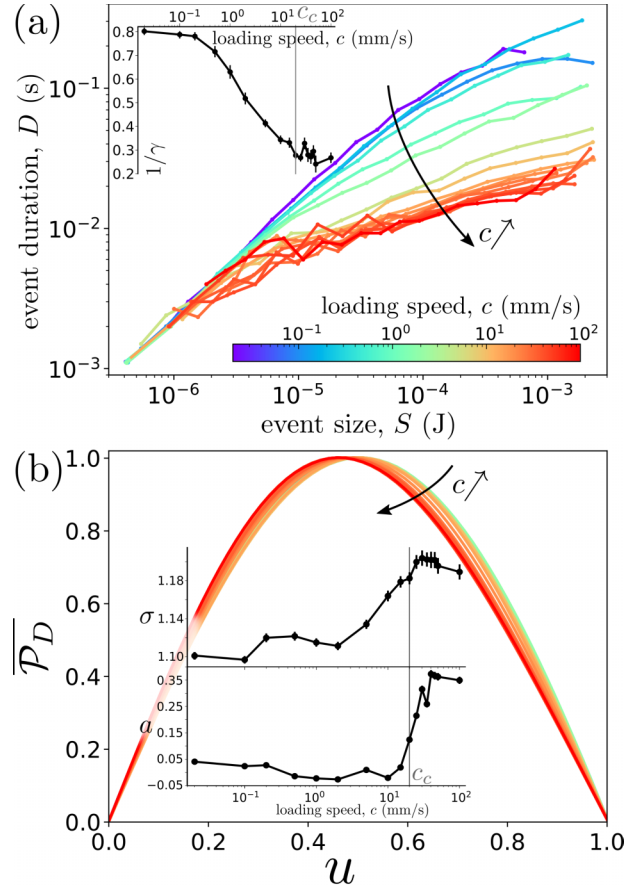


FIG. 4. (a) Evolution of avalanche duration,  $D(S)$ , for loading speeds  $c \in [0.02, 100]$  mm/s. Inset: Evolution of the exponent,  $1/\gamma$ . (b) Average shape  $\overline{P}_D$  for events with  $D_i \in [0.01, 0.02]$  s. Insets: Evolution of the exponent,  $\sigma$ , and asymmetry parameter,  $a$ , for event shapes as a function of  $c$  showing that events develop left-shifted asymmetry as  $c$  increases. In all graphs, error bars stand for 95% confidence level and vertical gray lines show  $c = c_c = 20$  mm/s.

for nominally brittle fracture in amorphous materials [5], we find that the productivity statistics and Båth's law can be directly implied from the Gutenberg-Richter law, without knowing the correct sequence of events. This fact disqualifies ETAS [36] for modeling our system.

The symmetric parabolic avalanche shape we observe in the crackling regime is predicted by many models [42], including the mean-field model [24]. In the periodic regime, however, we find asymmetric avalanche shapes with parameters different from those predicted by 3D simulations [23]. The source of the asymmetry is not clear, but we conjecture that it is related to a crossover in time scales associated with the slider motion and the relaxation dynamics of the granular bed. Moreover, we measure an exponent  $\sigma$  different from the value  $\gamma - 1$  predicted in Ref. [42]. This may be due to the combination of the physical effect of a finite driving rate and the experimental resolution that requires a finite threshold value for event detection. The former may yield overlapping avalanches that we classify as a single event, and the latter may result in the splitting of single avalanches into two or more events [46]. Similar features were observed in Barkhausen pulses [47] and were shown to result from the

finite value of the demagnetization factor. Further investigation of the grain scale dynamics during slip events is needed to clarify the origin of these macroscopic phenomena.

*Note added.* Bob Behringer passed away unexpectedly before this manuscript could be drafted. He played a crucial role in this work and his contribution clearly justifies inclusion as an author.

- 
- [1] J. P. Sethna, K. A. Dahmen, and C. R. Myers, Crackling noise, *Nature (London)* **410**, 242 (2001).
- [2] D. Bonamy, S. Santucci, and L. Ponson, Crackling Dynamics in Material Failure as the Signature of a Self-Organized Dynamic Phase Transition, *Phys. Rev. Lett.* **101**, 045501 (2008).
- [3] J. Barés, M. L. Hattali, D. Dalmas, and D. Bonamy, Fluctuations of Global Energy Release and Crackling in Nominally Brittle Heterogeneous Fracture, *Phys. Rev. Lett.* **113**, 264301 (2014).
- [4] H. V. Ribeiro, L. S. Costa, L. G. A. Alves, P. A. Santoro, S. Picoli, E. K. Lenzi, and R. S. Mendes, Analogies between the Cracking Noise of Ethanol-Dampened Charcoal and Earthquakes, *Phys. Rev. Lett.* **115**, 025503 (2015).
- [5] J. Barés, A. Dubois, L. Hattali, D. Dalmas, and D. Bonamy, Aftershock sequences and seismic-like organization of acoustic events produced by a single propagating crack, *Nat. Commun.* **9**, 1253 (2018).
- [6] W. F. Brace and J. D. Byerlee, Stick-slip as a mechanism for earthquakes, *Science* **153**, 990 (1966).
- [7] P. A. Johnson, H. Savage, M. Knuth, J. Gomberg, and C. Marone, Effects of acoustic waves on stick-slip in granular media and implications for earthquakes, *Nature (London)* **451**, 57 (2008).
- [8] J. S. Urbach, R. C. Madison, and J. T. Markert, Interface Depinning, Self-Organized Criticality, and the Barkhausen Effect, *Phys. Rev. Lett.* **75**, 276 (1995).
- [9] J. M. Beggs and D. Plenz, Neuronal avalanches in neocortical circuits, *J. Neurosci.* **23**, 11167 (2003).
- [10] T. Bellay, A. Klaus, S. Seshadri, and D. Plenz, Irregular spiking of pyramidal neurons organizes as scale-invariant neuronal avalanches in the awake state, *Elife* **4**, e07224 (2015).
- [11] P. Bak, K. Christensen, L. Danon, and T. Scanlon, Unified Scaling Law for Earthquakes, *Phys. Rev. Lett.* **88**, 178501 (2002).
- [12] J. Davidsen and G. Kwiatek, Earthquake Interevent Time Distribution for Induced Micro-, Nano-, and Picoseismicity, *Phys. Rev. Lett.* **110**, 068501 (2013).
- [13] F. Dalton and D. Corcoran, Self-organized criticality in a sheared granular stick-slip system, *Phys. Rev. E* **63**, 061312 (2001).
- [14] A. Baldassarri, F. Dalton, A. Petri, S. Zapperi, G. Pontuale, and L. Pietronero, Brownian Forces in Sheared Granular Matter, *Phys. Rev. Lett.* **96**, 118002 (2006).
- [15] A. Petri, A. Baldassarri, F. Dalton, G. Pontuale, L. Pietronero, and S. Zapperi, Stochastic dynamics of a sheared granular medium, *Eur. Phys. J. B* **64**, 531 (2008).
- [16] D. V. Denisov, K. A. Lőrincz, W. J. Wright, T. C. Hufnagel, A. Nawano, X. Gu, J. T. Uhl, K. A. Dahmen, and P. Schall, Universal slip dynamics in metallic glasses and granular matter—linking frictional weakening with inertial effects, *Sci. Rep.* **7**, 43376 (2017).
- [17] J. Barés, D. Wang, D. Wang, T. Bertrand, C. S. O’Hern, and R. P. Behringer, Local and global avalanches in a two-dimensional sheared granular medium, *Phys. Rev. E* **96**, 052902 (2017).
- [18] K. A. Murphy, K. A. Dahmen, and H. M. Jaeger, Transforming Granular Plasticity Through Particle Shape, *Phys. Rev. X* **9**, 011014 (2019).
- [19] A. Baldassarri, M. A. Annunziata, A. Gnoli, G. Pontuale, and A. Petri, Breakdown of scaling and friction weakening in the critical granular flow, [arXiv:1811.02464](https://arxiv.org/abs/1811.02464).
- [20] C. Maloney and A. Lemaitre, Subextensive Scaling in the Athermal, Quasistatic Limit of Amorphous Matter in Plastic Shear Flow, *Phys. Rev. Lett.* **93**, 016001 (2004).
- [21] K. M. Salerno, C. E. Maloney, and M. O. Robbins, Avalanches in Strained Amorphous Solids: Does Inertia Destroy Critical Behavior, *Phys. Rev. Lett.* **109**, 105703 (2012).
- [22] M. Otsuki and H. Hayakawa, Avalanche contribution to shear modulus of granular materials, *Phys. Rev. E* **90**, 042202 (2014).
- [23] C. Liu, E. E. Ferrero, F. Puosi, J.-L. Barrat, and K. Martens, Driving Rate Dependence of Avalanche Statistics and Shapes at the Yielding Transition, *Phys. Rev. Lett.* **116**, 065501 (2016).
- [24] K. A. Dahmen, Y. Ben-Zion, and J. T. Uhl, A simple analytic theory for the statistics of avalanches in sheared granular materials, *Nat. Phys.* **7**, 554 (2011).
- [25] M. Talamali, V. Petäjä, D. Vandembroucq, and S. Roux, Avalanches, precursors, and finite-size fluctuations in a mesoscopic model of amorphous plasticity, *Phys. Rev. E* **84**, 016115 (2011).
- [26] Z. Budrikis and S. Zapperi, Avalanche localization and crossover scaling in amorphous plasticity, *Phys. Rev. E* **88**, 062403 (2013).
- [27] J. Lin, E. Lerner, A. Rosso, and M. Wyart, Scaling description of the yielding transition in soft amorphous solids at zero temperature, *Proc. Natl. Acad. Sci. (USA)* **111**, 14382 (2014).
- [28] L. de Arcangelis, C. Godano, J. R. Grasso, and E. Lippiello, Statistical physics approach to earthquake occurrence and forecasting, *Phys. Rep.* **628**, 1 (2016).
- [29] D. F. Castellanos and M. Zaise, Avalanche Behavior in Creep Failure of Disordered Materials, *Phys. Rev. Lett.* **121**, 125501 (2018).
- [30] T. Utsu, Aftershocks and earthquake statistics (2): further investigation of aftershocks and other earthquake sequences based on a new classification of earthquake sequences, *J. Faculty Sci., Hokkaido Univ., Ser. 7 Geophys.* **3**, 197 (1971).
- [31] A. Helmstetter, Is Earthquake Triggering Driven by Small Earthquakes, *Phys. Rev. Lett.* **91**, 058501 (2003).
- [32] M. Båth, Lateral inhomogeneities of the upper mantle, *Tectonophysics* **2**, 483 (1965).
- [33] F. Omori, On after-shocks of earthquakes, *J. Coll. Sci. Imp. Univ. Tokyo* **7**, 111 (1894).

## ACKNOWLEDGMENTS

We gratefully acknowledge fruitful discussions with Kirsten Martens and Daniel Bonamy. The work was supported by NSF Grants No. DMR-1206351 and No. DMR-1809762, NASA Grant No. NNX15AD38G, the William M. Keck Foundation, and DARPA Grant No. 4-34728.

- [34] T. Utsu, Aftershocks and earthquake statistics (3): Analyses of the distribution of earthquakes in magnitude, time and space with special consideration to clustering characteristics of earthquake occurrence (1), *J. Faculty Sci., Hokkaido Univ., Ser. 7 Geophys.* **3**, 379 (1972).
- [35] T. Utsu, Y. Ogata, and R. S. Matsu'ura, The centenary of the Omori formula for a decay law of aftershock activity, *J. Phys. Earth* **43**, 1 (1995).
- [36] Y. Ogata, Statistical models for earthquake occurrences and residual analysis for point processes, *J. Am. Stat. Assoc.* **83**, 9 (1988).
- [37] J. Krim, P. Yu, and R. P. Behringer, Stick-slip and the transition to steady sliding in a 2d granular medium and a fixed particle lattice, *Pure Appl. Geophys.* **168**, 2259 (2011).
- [38] A. A. Zadeh, J. Barés, and R. P. Behringer, Crackling to periodic dynamics in granular media, *Phys. Rev. E* **99**, 040901(R) (2019).
- [39] A. Helmstetter and D. Sornette, Båth's law derived from the Gutenberg-Richter law and from aftershock properties, *Geophys. Res. Lett.* **30**, 1576 (2003).
- [40] A. A. Zadeh, J. Barés, and R. P. Behringer, Avalanches in a granular stick-slip experiment: detection using wavelets, *EPJ Web Conf.* **140**, 03038 (2017).
- [41] J. Barés, M. Barlet, C. L. Rountree, L. Barbier, and D. Bonamy, Nominally brittle cracks in inhomogeneous solids: from microstructural disorder to continuum-level scale, *Front. Phys.* **2**, 70 (2014).
- [42] L. Laurson, X. Illa, S. Santucci, K. T. Tallakstad, K. J. Måløy, and M. J. Alava, Evolution of the average avalanche shape with the universality class, *Nat. Commun.* **4**, 2927 (2013).
- [43] J. Baró, A. Corral, X. Illa, A. Planes, E. K. H. Salje, W. Schranz, D. E. Soto-Parra, and E. Vives, Statistical Similarity Between the Compression of a Porous Material and Earthquakes, *Phys. Rev. Lett.* **110**, 088702 (2013).
- [44] S. Lherminier, R. Planet, G. Simon, K. J. Måløy, L. Vanel, and O. Ramos, A granular experiment approach to earthquakes, *Rev. Cub. Fís.* **33**, 55 (2016).
- [45] P. D. Ispánovity, L. Laurson, M. Zaiser, I. Groma, S. Zapperi, and M. J. Alava, Avalanches in 2d Dislocation Systems: Plastic Yielding Is Not Depinning, *Phys. Rev. Lett.* **112**, 235501 (2014).
- [46] S. Janičević, L. Laurson, K.-J. Måløy, S. Santucci, and M. J. Alava, Interevent Correlations from Avalanches Hiding Below the Detection Threshold, *Phys. Rev. Lett.* **117**, 230601 (2016).
- [47] S. Papanikolaou, F. Bohn, R. L. Sommer, G. Durin, S. Zapperi, and J. P. Sethna, Universality beyond power laws and the average avalanche shape, *Nat. Phys.* **7**, 316 (2011).